Published in final edited form as:
Cell Host Microbe. 2008 December 11; 4(6): 567–578. doi:10.1016/j.chom.2008.11.001.

The Fatty Acid Biosynthesis Enzyme FabI Plays a Key Role In the Development of Liver Stage Malarial Parasites

Min Yu[1,2,¶], **T. R. Santha Kumar**[1,2,¶], **Louis J. Nkrumah**[2], **Alida Coppi**[3], **Silke Retzlaff**[4], **Celeste D. Li**[1], **Brendan J. Kelly**[5], **Pedro A. Moura**[1], **Viswanathan Lakshmanan**[2,†], **Joel S. Freundlich**[6], **Juan-Carlos Valderramos**[1], **Catherine Vilcheze**[2], **Mark Siedner**[5], **Jennifer H.-C. Tsai**[6], **Brie Falkard**[1], **Amar bir Singh Sidhu**[1], **Lisa A. Purcell**[1,≠], **Paul Gratraud**[7], **Laurent Kremer**[7,8], **Andy P. Waters**[9], **Guy Schiehser**[10], **David P. Jacobus**[10], **Chris J. Janse**[11], **Arba Ager**[12], **William R. Jacobs Jr.**[2,13], **James C. Sacchettini**[6], **Volker Heussler**[4], **Photini Sinnis**[3], and **David A. Fidock**[1,5,*]

[1] *Department of Microbiology, Columbia University, New York, NY 10032, USA* [2] *Department of Microbiology and Immunology, Albert Einstein College of Medicine, Bronx, NY 10461, USA* [3] *Department of Medical Parasitology, New York University School of Medicine, New York, NY 10010, USA* [4] *Bernhard Nocht Institute for Tropical Medicine, Hamburg, Germany* [5] *Department of Medicine, Columbia University, New York, NY 10032, USA* [6] *Department of Biochemistry and Biophysics, Texas A&M University, College Station, TX 77843, USA* [7] *Universités de Montpellier II and I, CNRS UMR5235* [8] *INSERM, DIMNP, Montpellier, France* [9] *Wellcome Centre for Molecular Parasitology, University of Glasgow, Scotland, UK* [10] *Jacobus Pharmaceutical Company, Princeton, NJ 08540, USA* [11] *Department of Parasitology, Centre of Infectious Diseases, Leiden University, The Netherlands* [12] *Department of Microbiology and Immunology, University of Miami, Miami, FL 33177, USA* [13] *Howard Hughes Medical Institute, Albert Einstein College of Medicine, Bronx, NY 10461, USA*

SUMMARY

Fatty acid biosynthesis has been viewed as an important biological function of and therapeutic target for *Plasmodium falciparum* asexual blood stage infection. This apicoplast-resident type II pathway, distinct from the mammalian type I process, includes FabI. Here, we report synthetic chemistry and transfection studies concluding that *Plasmodium* FabI is not the target of the antimalarial activity of the bacterial FabI inhibitor triclosan. Disruption of *fabI* in *P. falciparum* or the rodent parasite *P. berghei* does not impede blood stage growth. In contrast, mosquito-derived *fabI*-deficient *P. berghei* sporozoites are markedly less infective for mice and typically fail to complete liver stage development *in vitro*. This is characterized by an inability to form intra-hepatic merosomes that normally initiate blood stage infections. These data illuminate key differences between liver and blood stage parasites in their requirements for host versus *de novo* synthesized fatty acids, and create new prospects for stage-specific antimalarial interventions.

*Corresponding author: df2260@columbia.edu; Tel: +1 212 305 0816; FAX: +1 212 305 4038.
¶These authors contributed equally to this work.
†Current Address: Department of Molecular Biology, Princeton University, Princeton, NJ 08544, USA
≠Current Address: Regeneron, Tarrytown, NY 10591, USA

INTRODUCTION

Plasmodium parasites must coordinate the salvage of host factors with *de novo* biosynthesis pathways in order to meet the unique demands of each intracellular stage of their life cycle. In mammals, this begins with the bite of an infected *Anopheles* mosquito. The intradermally injected sporozoites (SPZ) then migrate to the liver and invade hepatocytes (Amino et al., 2008). Liver stage development involves the transformation of an intracellular sporozoite, bounded by an inner parasite plasma membrane (PPM) and an outer parasitophorous vacuolar membrane (PVM), into a liver stage trophozoite. This stage undergoes prolific nuclear division and membrane synthesis, with commensurate metabolic demands. In the case of *P. falciparum*, the most lethal etiologic agent of human malaria, each infected hepatocyte produces up to 10,000–30,000 merozoites, contained within an intra-hepatic merosome, over 6–7 days.

Liberated liver stage merozoites enter the bloodstream where they invade red blood cells (RBC) and initiate the asexual blood stages that cause clinical manifestations of disease. Parasite development inside these anucleate cells displays several fundamental differences from the liver stages (Silvie et al., 2008b). These include the ability of asexual blood stage parasites to degrade hemoglobin and detoxify heme (processes that are key to the mode of action of multiple antimalarials), and also to modify the host cell membrane such that the infected RBC can sequester in the microvasculature. The entire asexual cycle is completed within 48 hr, producing 8–24 infectious merozoites per infected RBC. In contrast to the small liver stage inoculum, numbers of infected RBC can exceed 10^{12} per host (Greenwood et al., 2008). Intra-erythrocytic parasites can also transform into sexual gametocyte stages. Upon their ingestion by a feeding *Anopheles* mosquito, these parasites undergo fertilization and sexual recombination, ultimately producing oocyst SPZ that migrate to the salivary glands, ready to initiate a new round of infection.

The prodigious proliferative capacity of malarial parasites necessitates access to an abundant source of fatty acids (FA). These carboxylic acid-linked acyl chains are required for the production of lipid species that are essential for parasite membrane and lipid body biogenesis (Palacpac et al., 2004). FA are also required for glycosylphosphatidylinositol (GPI) moieties that serve to anchor parasite membrane proteins (Gilson et al., 2006). FA and phospholipid concentrations are respectively 6–fold and 3 to 5–fold higher in infected compared to uninfected RBC. This was initially attributed to FA salvage from host plasma, as parasites were thought to be incapable of *de novo* synthesis (Vial and Ancelin, 1992). The paradigm changed with the discovery that *P. falciparum* harbors components of a type II FA biosynthesis (FAS-II) pathway (Ralph et al., 2004). A subsequent study reported that *P. falciparum* asexual blood stages had FAS-II activity, producing FA with chain lengths of C_{10} to C_{14} (Surolia and Surolia, 2001). FAS-II enzymes have been localized to the apicoplast, a non-photosynthetic plastid organelle of cyanobacterial origin. In addition to FA biosynthesis, the apicoplast harbors unique pathways for the synthesis of isoprenoids and heme, and shares lipoic acid synthesis and salvage pathways with the mitochondria. The discovery that antibiotics with antimalarial activity inhibit apicoplast function has highlighted the therapeutic potential of targeting this organelle (Ralph et al., 2004).

The FAS-II pathway in *Plasmodium* has been of particular therapeutic interest because it is distinct from the type I (FAS-I) pathway found in mammals. FAS-II requires acetyl-Coenzyme A (CoA), which can be converted from pyruvate by the pyruvate dehydrogenase complex. Acetyl-CoA carboxylase converts acetyl-CoA to malonyl-CoA, which is tethered to an acyl carrier protein (ACP) by malonyl-CoA:ACP transacylase (FabD). This produces malonyl-ACP, which in conjunction with acetyl-CoA is acted upon by β-ketoacyl-ACP synthase III (Fab H) to form β-ketoacyl-ACP. This precursor enters the FAS-II elongation cycle, mediated

by FabB/F (β-ketoacyl-acyl-carrier-protein (ACP) synthase), FabG (β-ketoacyl-ACP reductase), FabZ/A (β-hydroxyacyl-ACP dehydratase) and FabI (*trans*-2-enoyl-ACP reductase). These four FAS-II enzymes iteratively catalyze the addition of two carbon chains to a growing fatty acyl carbon chain, via condensation, reduction, dehydration and reduction steps, respectively. In contrast, FAS-I contains all four enzymatic functionalities within a single, large polypeptide (Mazumdar and Striepen, 2007).

Studies from pathogenic bacteria have confirmed the therapeutic value of FAS-II inhibitors (Zhang et al., 2006). These include triclosan, a microbicide widely used in consumer products. A highly cited report describing triclosan antimalarial activity *in vitro* against *P. falciparum* and *in vivo* against the rodent parasite *P. berghei*, directed against the pathogenic asexual blood stages, generated tremendous interest in this compound and its predicted target - FabI (Surolia and Surolia, 2001). This led to the structural elucidation of the *P. falciparum* FabI (PfFabI; PlasmoDB gene ID PFF0730c) homotetramer to which triclosan:NAD^+ adducts bind in the active site, and propelled structure-guided efforts to develop novel antimalarials based on triclosan (Freundlich et al., 2007; Muralidharan et al., 2003; Perozzo et al., 2002). Here, we report our investigations into a series of analogs designed to improve on the antimalarial properties of triclosan and our ensuing studies that focused on the biological role of FabI.

RESULTS

Triclosan Activity Against *Plasmodium* Asexual Blood Stages Does Not Correlate With its Inhibition of Purified Recombinant FabI

We initiated a structure-guided medicinal chemistry program to improve the potency of triclosan by modifying substituents around its diaryl ether scaffold. This led us to synthesize 80 analogs (Figure 1A), for which only a single position was modified to reduce the likelihood of creating off-target activity. These analogs, grouped by the carbon position that was modified (see Figure 1B inset; detailed in Table S1 in the Supplemental Data available with this article online), were evaluated for their inhibition of cultured *P. falciparum* asexual blood stage parasites (3D7 and Dd2 lines), and separately, for inhibition of purified PfFabI enzyme. Activities were compared against triclosan, which yielded mean IC_{50} values of 1.8 μM and 2.1 μM against the 3D7 and Dd2 lines and an EC_{50} value of 73 nM against purified PfFabI. Individual analog series showed substantial differences in their inhibitory activities (Figure 1A). The 2′-position analog series afforded the most potent inhibitors in the parasite assays, yet showed minimal inhibition of PfFabI. Modifications at the 4′- or 5- position afforded a few modest improvements in efficacy, mostly against PfFabI, whereas changes at the 4- or 6-position generally produced less potent inhibitors. We also noted that compound series with similar mean potencies against PfFabI (e.g. the 4′- and 5- position analogs) exhibited nearly 10–fold differences in their mean antiparasitic activities. Further analysis revealed a lack of a significant association between enzyme and parasite inhibition, as evidenced by the Pearson r^2 values of 0.13 and 0.15 obtained by plotting these data for 3D7 and Dd2 respectively (Figure 1B; data not shown). While chemical properties such as membrane permeability and solubility might obscure close whole-cell and enzyme correlations for on-target compounds, our data nonetheless raised doubts that triclosan analogs acted against asexual blood stage parasites by inhibiting PfFabI.

In parallel with these studies, we re-evaluated the *in vivo* efficacy of triclosan. A previous report had documented that four days of subcutaneous injections of triclosan at 3 mg/kg/day could suppress *P. berghei* parasitemia by 75%, and that injections with doses of 38 mg/kg/day cured the infected mice with 100% efficacy (Surolia and Surolia, 2001). We tested both oral (PO) and subcutaneous (SC) routes of triclosan, administered over a range of 16 to 512 mg/kg/day, for three days with a twice-daily divided dose, to mice infected three days prior with *P. berghei* (KBG-173 line). Parasitemias were recorded on day 6 post-infection (i.e. one day after

the last dose of triclosan) and were 61% or 57% (for PO or SC respectively) in control (infected and placebo-treated) mice. Increasing the triclosan concentrations from 16 to 128 mg/kg/day caused a dose-dependent decrease in parasitemias, to a minimum of 27% or 13% with 128 mg/kg/day triclosan administered PO or SC respectively (Figure 1C). Higher doses failed to further suppress the parasitemias.

Assessment of survival showed that all control mice died by days 10 (PO) or 12 (SC) (Figure 1D, E). Oral administration of 64 mg/kg/day triclosan yielded a slight extension in survival times, and doses of 128 or 256 mg/kg/day produced 30% survival rates measured at day 31. Increasing the dose to 512 mg/kg/day led to some early mortality and decreased overall survival rates, suggesting some toxicity. Via the SC route, triclosan was moderately more effective, although survival never exceeded 50%. *In vivo* tests with several analogs (compounds 18, 20, 22, 41, 45 & 60 in Table S1), whose *in vitro* potencies were comparable to triclosan, revealed no improvements over the parent compound (A. Ager and D. Jacobus, unpublished data). We concluded that, under our experimental conditions, triclosan had reduced antimalarial potency *in vivo* as compared to the earlier report (Surolia and Surolia, 2001). Furthermore, the *in vitro* potency of triclosan analogs did not correlate with their inhibition of FabI enzymatic activity.

Transgene Expression of a Mutant FabI That is Biochemically Resistant to Triclosan Does Not Decrease *P. falciparum* Susceptibility to This Agent

To further investigate the role of FabI in the mode of action of triclosan, we transfected *P. falciparum* asexual blood stage parasites with plasmids expressing V5 epitope-tagged forms of *pffabI* that were either wild type (WT) or that encoded the A217V mutation. This mutation was selected because it confers a 7,000-fold decrease in triclosan binding affinity for recombinant PfFabI (Kapoor et al., 2004). To express these *pffabI* transgenes, we selected the *calmodulin* (PF14_0323) promoter, which is highly active in asexual blood stages (www.PlasmoDB.org). Integration of these plasmids (named *pffabI*(A217V)-V5-attP and *pffabI*(WT)-V5-attP; Table 1) into the *P. falciparum* genome was achieved using the Bxb1 serine integrase-mediated attBxattP system of recombination, which delivers transgenes into the attB-marked *cg6* locus and results in a genetically and phenotypically homogeneous population of recombinant parasite lines (Nkrumah et al., 2006). The transfections, performed with $Dd2^{attB}$ and $3D7^{attB}$ parasites, produced the transgenic lines Pf*fabI*$(A217V)^{Dd2}$, Pf*fabI*$(WT)^{Dd2}$, Pf*fabI*$(A217V)^{3D7}$ and Pf*fabI*$(WT)^{3D7}$ (Table 1; Figure S1A). Southern blot analysis confirmed correct integration of the *pffabI* transgenic copies into the *cg6*-attB site and the predicted organization of the endogenous *pffabI* locus (Figure S1B; data not shown). Western blot analysis with anti-V5 antibodies revealed the expression of ~46 kDa V5-tagged PfFabI proteins in all four lines (Figure S1C). Immunofluorescence assays with the Pf*fabI*$(A217V)^{Dd2}$ line showed co-localization of PfFabI-V5 and the apicoplast-resident acyl carrier protein (ACP) in a compartment distinct from the nucleus (stained with Hoechst 33342) and the mitochondrion (stained with MitoTracker Red), thus confirming trafficking of V5-tagged PfFabI to the apicoplast (Figure 2A, B). We proceeded to measure the triclosan susceptibility of our transgenic and parental lines. Results from drug susceptibility assays showed no significant difference in either IC_{50} or IC_{90} values between recombinant lines expressing mutant or WT PfFabI (Figure 2C; values provided in legend).

P. falciparum FabI is Not Expressed at Detectable Levels in Asexual Blood Stage Parasites

Subsequent Northern blot experiments detected the presence of *pffabI* transcripts only in the transgenic lines (Pf*fabI*$(A217V)^{Dd2}$, Pf*fabI*$(WT)^{Dd2}$, Pf*fabI*$(A217V)^{3D7}$ and Pf*fabI*$(WT)^{3D7}$) that express an additional *pffabI* copy from the highly active mature stage *calmodulin* promoter, and not in the lines expressing endogenous *pffabI* alone ($Dd2^{attB}$, Dd2, $3D7^{attB}$ and 3D7; Figure 2D). We attribute the apparent increase in *pffabI* transcripts in the Pf*fabI*$(A217V)^{Dd2\ and}$

Pf*fabI*(A217V)^{3D7} lines, compared to the Pf*fabI*(WT)^{Dd2} and Pf*fabI*(WT)^{3D7} lines, to the higher proportions of mature stage parasites in the former at the time of RNA harvest. To confirm the lack of endogenous *pffabI* expression at the protein level, we raised rabbit polyclonal antiserum against purified recombinant PfFabI. Western blot analysis with extracts of parasites expressing *calmodulin* promoter-driven PfFabI-V5 showed that the antiserum and monoclonal antibodies against the V5 epitope tag both detected a ~46 kDa protein (Figure 2E). The anti-PfFabI antiserum did not detect any protein in extracts of control parasites expressing *pffabI* from its endogenous promoter (Figure 2F).

FabI is Not Required for Normal Propagation of *P. falciparum* Asexual Blood Stage Parasites and its Absence Does Not Alter Parasite Susceptibility to Triclosan

These findings led us to question whether *pffabI* is required for *P. falciparum* asexual blood stage growth *in vitro*. To test this, we designed a DNA construct (pcam-*bsd*-Δ*pffabI*), which contained an internal region of the *pffabI* coding sequence (encoding amino acids 98 to 295) such that homologous recombination between this fragment and the endogenous *pffabI* gene would separate the full-length sequence into two truncated fragments (Figure S2A). The upstream fragment lacked the 3′ end of the gene corresponding to amino acids 296–432 (thereby eliminating the β6–β9 helices and β6–β7 strands that contribute to forming the NADH-binding Rossman fold). The downstream fragment lacked a promoter and the first 98 amino acids that included the bipartite targeting sequence predicted to be required for protein trafficking to the apicoplast (Perozzo et al., 2002). Transfection of cultured Dd2 parasites with this knockout construct resulted in the generation of parasite clones (Pf*Δfabl*^{1} and Pf*Δfabl*^{2}) in which the *pffabI* gene had been disrupted by single site crossover and plasmid integration, as confirmed by PCR and Southern blot analyses (Table 1; Figure S2B, C). Measurements of parasitemia over a two-month period revealed equivalent growth rates (averaging 5.0 to 5.6–fold multiplication per 48 hr cycle of RBC invasion, intracellular development and egress) between these knockout clones and parental Dd2. These data demonstrated the non-essentiality of *pffabI* for asexual blood stage propagation, and implied that the activity of triclosan against these stages could not result from inhibition of PfFabI. This was confirmed with drug susceptibility assays that revealed similar triclosan susceptibilities in Pf*Δfabl*^{1}, Pf*Δfabl*^{2} and the parental Dd2 line (mean ± SEM IC_{50} values of 2.2±0.2, 2.4±0.3 and 2.1±0.3 μM respectively, derived from three separate experiments performed in duplicate).

Deletion of *P. berghei fabI*, the *pffabI* Ortholog, Does Not Affect Propagation of Blood Stage Parasites *In Vivo*

Our *P. falciparum in vitro* data led us to examine whether this protein was essential for proliferation of asexual blood stages *in vivo*. For this, we used the highly virulent *P. berghei* ANKA rodent malaria model. Comparisons of the amino acid sequences of PfFabI and its predicted ortholog in *P. berghei*, PbFabI (PB000088.02.0), revealed 62% identity and 74% similarity (Figure S3A). Bacterial expression and purification of PbFabI enabled us to elucidate its structure at 2.5Å resolution. Superimposing this with the known PfFabI structure (Perozzo et al., 2002) revealed a nearly identical organization with each subunit in the tetramer containing 9 α-helices and 7 β-sheets (Figure S3B). Detailed inspection of the active sites revealed these to be indistinguishable (Figure S3C). From these studies, we can confidently predict that PbFabI and PfFabI fulfill the same enzymatic function for *Plasmodium* parasites.

We transfected *P. berghei* ANKA parasites with a DNA construct termed pLitmus28-Δ*pbfabI*. This was designed to permit double crossover, resulting in complete deletion of the endogenous *pbfabI* locus and its replacement by the *T. gondii* dihydrofolate reductase-thymidylate synthase (*Tgdhfr-ts*) selectable marker that confers resistance to pyrimethamine. From this transfection, we selected mutant parasites and used limiting dilution to obtain a clone, termed Pb*Δfabl* (Table 1). PCR and Southern blot analyses confirmed correct integration of

the DNA construct and deletion of the *pbfabI* coding sequence in this clone (Figure S4A, C, D). As a "knock-in" control, we utilized a similar double crossover strategy to replace the endogenous gene with a construct that reinserted a full-length, functional *pbfabI* gene under control of the endogenous promoter, as well as the *Tgdhfr-ts* selectable marker. This yielded the Pb*fabI*^{Rec} clone, whose recombinant locus was confirmed by PCR and Southern blot hybridization (Figure S4B, C, D). Measurements of parasitemia in mice infected with PbΔ*fabI*, Pb*fabI*^{Rec} or parental ANKA revealed similar rates of proliferation, calculated to be 4.8±1.4, 5.5±2.2 and 4.4±1.7 per 24 hr cycle respectively in two comparative experiments with groups of 4 mice each (values represents means±SD; Figure S4E). These values were not statistically different between lines, as determined by Mann-Whitney tests. Thus, there was no substantial decrease in asexual blood stage *in vivo* viability upon deletion of *pbfabI*.

Drug susceptibility assays with *P. berghei* asexual blood stages tested *ex vivo* showed equivalent triclosan IC_{50} values in the PbΔ*fabI*, Pb*fabI*^{Rec} and ANKA lines (means±SEM of 1.4±0.1, 1.5±0.2 and 1.2±0.1 μM respectively). Control assays with the unrelated antimalarial chloroquine produced IC_{50} values of 11.0±0.1, 13.0±0.6 and 10.4±0.3 nM in these lines respectively. These results, combined with the *P. falciparum* studies, conclusively demonstrate that the blood stage activity of triclosan is not attributable to inhibition of FabI.

Plasmodium Asexual Blood Stage Parasites Lacking FabI Can Produce FA Species

The availability of parasite lines lacking FabI allowed us to determine whether *Plasmodium* asexual blood stages utilize the FAS-II pathway to synthesize FA *de novo*. We incubated synchronized trophozoite stage *P. falciparum* and *P. berghei* control and *fabI* knockout parasites with [^{14}C]-labeled acetate, a radiolabeled FA precursor, then extracted the free FA that had incorporated this substrate and analyzed them by reversed-phase High Performance Liquid Chromatography (HPLC). In *P. falciparum*, this led us to detect radiolabeled C_{16} and C_{18} FA in both the Pf*fabI*^{1} and Dd2 lines (Figure 3A, B). Thus, extension of FA could occur in the absence of the key FAS-II enzyme FabI. In a separate experiment, we incubated Pf*fabI*^{1} and other *P. falciparum* lines with [^{14}C]-labeled acetate, extracted their FA and analyzed them by reversed-phase thin layer chromatography. This confirmed the production of radiolabeled C_{16} and C_{18} independently of FabI (Figure S2D). We note that these findings are in contrast with an earlier report that *P. falciparum* asexual blood stage parasites synthesize C_{10} to C_{14} FA (Surolia and Surolia, 2001).

[^{14}C]-acetate incorporation studies with the *P. berghei* lines produced evidence of *de novo* FA elongation with PbΔ*fabI* parasites, with no visible difference between the PbΔ*fabI* and parental ANKA lines in terms of the lengths of FA that were produced (Figure 3C, D). In contrast to *P. falciparum*, the rodent parasites synthesized FA chain lengths of C_{12} to C_{24}. No radiolabeled FA were observed with rodent or human uninfected RBC controls (data not shown). These data provide evidence that the two *Plasmodium* species differ in the range of FA that they can extend *de novo*; yet they share the common characteristic that FabI is not required.

P. berghei Sporozoites Lacking FabI Are Markedly Attenuated in Their Ability to Progress to Asexual Blood Stage Infections

The availability of a *P. berghei* line (PbΔ*fabI*) lacking FabI made it possible to explore the role of this protein in other stages of the parasite life cycle. We observed that gametocyte production, gamete fertilization, and the subsequent development of ookinetes and oocysts appeared unaffected by the absence of FabI, as judged by the similar numbers of oocysts that developed in *Anopheles stephensi* mosquitoes fed on mice infected with the PbΔ*fabI*, Pb*fabI*^{Rec} or ANKA lines (data not shown). In two separate experiments, we observed no difference in the numbers of oocyst and salivary gland SPZ produced by these lines (data not shown).

To determine whether FabI plays a role in the infectivity of SPZ to the mammalian host, salivary gland SPZ were dissected and inoculated into the tail vein of C57BL/6 mice. This inbred strain of mouse was chosen as it is more susceptible than other inbred or outbred mouse strains to *P. berghei* SPZ infections (Scheller et al., 1994). Experiments were performed on three separate occasions and were highly reproducible. Intravenous injections of 1,000 ANKA or Pb*fabI*^{Rec} SPZ produced patent blood stage infections that were microscopically detectable in 16/16 and 15/15 mice by day five (Table 2). In contrast, injection of 1,000 PbΔ*fabI* SPZ produced a blood stage infection in only 5/16 mice, with the infected mice showing a delay in patency of 4 days. Increasing the PbΔ*fabI* inoculum to 10,000 SPZ resulted in patent infections in 13/15 mice, with those mice again showing an average delay of 4 days compared to controls.

We also assayed the infectivity of SPZ delivered by mosquito bite, to test for any defect in SPZ tissue traversal and migration from the dermis to the liver (Silvie et al., 2008b). Groups of 20 infected mosquitoes were allowed to feed on each mouse, with 5 mice tested per *P. berghei* line. Based on earlier studies, we estimate that each infected mosquito intradermally delivers ~120 SPZ (Medica and Sinnis, 2005), yielding an approximate inoculum of 2,000 SPZ. Results showed that each mouse infected with ANKA or Pb*fabI*^{Rec} parasites, as well as 4 of the 5 mice infected with PbΔ*fabI* SPZ, developed a patent blood stage infection. However, the latter group showed a 5-day delay (Table 2).

Taken together, the data demonstrate that *P. berghei* parasites lacking FabI produce SPZ that are highly attenuated in their infectivity to the mammalian host. We note that all "breakthrough" PbΔ*fabI* asexual blood stage infections became fulminant and lethal by days 20–29. This suggests that once PbΔ*fabI* parasites developed into blood stages, they showed no loss of virulence compared to WT parasites. PCR analysis of breakthrough infections confirmed that they resulted from PbΔ*fabI* parasites, and not from contamination with ANKA or Pf*fabI*^{Rec} parasites (Figure S4F).

PbΔ*fabI* Sporozoites Typically Fail to Produce Infectious Mature Liver Stage Parasites

To investigate the cause of this decreased infectivity of PbΔ*fabI* SPZ, we first examined cell traversal and invasion of hepatocytes. The former occurs when SPZ transit through cells prior to initiating liver stage development by forming a parasitophorous vacuole inside the invaded cell (Silvie et al., 2008b). In two independent experiments, rates of cell traversal were similar, with a mean of 9–13 dextran positive (i.e. traversed) cells per field. PbΔ*fabI* and Pb*fabI*^{Rec} lines were also found to be equally competent for invasion, with 34–38% success in invading Hepa 1–6 cells. We next assessed the maturing liver stage parasites. At 24, 36 or 48 hr post-invasion, PbΔ*fabI* and Pb*fabI*^{Rec} parasites stained with antibodies specific for the *P. berghei* cytosolic protein HSP70 (PB000817.02.0) showed equivalent numbers and developmental stages (data not shown). We also tested for *fabI* transcription in these stages. RT-PCR studies from infected Hepa 1–6 cells harvested 40 hr post-invasion revealed *pbfabI* mRNA transcripts in Pb*fabI*^{Rec} but not PbΔ*fabI* liver stage parasites (Figure S4G). These results indicate that *fabI* is normally transcribed by liver stage parasites, however the lack of expression in PbΔ*fabI* parasites did not affect SPZ cell traversal, invasion of hepatocytes, or the initial stages of intra-hepatic development.

We proceeded to investigate later stages of liver stage maturation using the HepG2 hepatoma cell line, which is able to support SPZ invasion and liver stage development through to the production of merozoites that are infectious for RBC. Immunofluorescence assays (IFAs) with mature hepatic stages were performed with antibodies that recognize the *P. berghei* parasite proteins Exp1 (PB000484.01.0) or MSP1 (PB000172.01.0). Exp1 is expressed throughout trophozoite development and schizogony and is exported into the parasitophorous vacuolar membrane (PVM) that separates the parasite from the host cell cytosol. In late liver stages, the Exp1-positive PVM is typically observed as a closed circular structure around the multiplying

parasite nuclei (Sturm et al., 2006). In schizont stages, MSP1 is expressed and becomes integrated into the parasite plasma membrane (PPM). The PPM invaginates around pockets of parasite material during the cytomere stage, and ultimately forms the membrane of individual merozoites (Sturm et al., 2008).

These antibodies revealed a striking difference between ANKA and Pb*Δfabl* parasites very late in their liver stage development. At 60 hr post SPZ invasion of HepG2 cells, 59% of the ANKA parasites were found to have developed into an advanced parasite stage marked by MSP1-positive PPM invaginations (Figure 4A; Figure S5A). Many of these parasites were observed at the cytomere stage in which the PPM surrounded large groups of parasite nuclei (see row 2 in Figure S5A). The remaining 41% of parasites were MSP1-negative, indicating either delayed or aberrant development. In contrast, almost all Pb*Δfabl* liver stage parasites (99.5%) were negative for MSP1 staining, despite having initiated their development inside an Exp1-positive PVM (Figure 4A). In addition to the lack of MSP1 expression in Pb*Δfabl* parasites, nuclear division was clearly impeded, as evidenced by the limited number of DAPI-positive parasite nuclei (Figure 4A). The very few MSP1-positive Pb*Δfabl* liver stage parasites that we did observe were restricted in size, with minimal PPM invaginations (Figure 4A; Figure S5A). In support of this, at 60–65 hr post-invasion we recorded no cytomere stage in over 3,500 Pb*Δfabl* liver stage parasites, whereas cytomeres were observed in 266 ANKA parasites out of a total of 3,366. At these late stages of parasite development, ANKA parasites began to degrade the PVM, as evidenced by their lack of the typical Exp1-positive closed circular structures seen in earlier stages (Figure S5B). This resulted in the generation of large clusters of MSP1-positive merozoites that filled the entire hepatocyte cytoplasm. Of these PVM-degraded ANKA-infected cells, 87% contained MSP1-positive merozoites. The remaining 13% were MSP1-negative, suggesting that these had undergone aberrant development and had failed to produce viable merozoites (Figure S5B). In contrast, every Pb*Δfabl* parasite that was found to have a non-intact PVM was MSP1-negative and was not producing mature merozoites (Figure S5B).

At the 65 hr time point, we also recorded the numbers of infected cells that had detached from the monolayer into the culture supernatant. These so-called “detached cells” harbor merozoites that have been released into the host cell cytoplasm following normal degradation of the PVM (Sturm et al., 2006). In three independent experiments, we did not observe a single detached cell with the Pb*Δfabl* parasites. In contrast, detached cells numbered 210, 236 and 106 with ANKA parasites and 298, 136 and 103 with Pb*fabl*^{Rec} parasites (Figure 4B). From these cultures, we also recorded the number of merosomes, i.e. the membrane-bound clusters of merozoites devoid of host nuclei that egress from the infected hepatocytes (Sturm et al., 2006; Sturm et al., 2008). Merosomes were never observed in Pb*Δfabl* liver stage cultures in any of these three experiments. By comparison, ANKA parasites produced 69, 174 and 41 merosomes, while Pb*fabl*^{Rec} parasites produced 77, 68 and 13 merosomes respectively (Figure 4B). Similar results were obtained in three additional experiments that examined liver stage parasites 70 hr post-invasion (data not shown), confirming a key role for FabI during the final maturation of the liver stage schizont and the formation of merozoites.

While we never observed Pb*Δfabl* merosomes, even after an extended culture period of 90 hr, we nevertheless recorded rare instances of MSP1-positive Pb*Δfabl* merozoites. We also observed one instance of a cytomere stage at 70 hr post-invasion. The formation of these few merozoites and their passage into the blood stream might account for the Pb*Δfabl* breakthrough blood stage infections observed *in vivo*.

DISCUSSION

Here we report on the discovery that the FAS-II enzyme FabI plays a key role in the development of infectious liver stage merozoites. Our study reveals a fundamental difference in how *Plasmodium* liver and asexual stage parasites balance *de novo* synthesis and salvage of host factors to meet their FA requirements for intracellular parasite propagation. For asexual blood stages, our findings provide evidence against a recent report of an active FAS-II pathway (Surolia and Surolia, 2001), and instead support an alternate mechanism of FA modification that appears to act alongside a predominant import pathway.

The asymptomatic liver stage begins with SPZ productively infecting hepatocytes (Mikolajczak and Kappe, 2006; Prudencio et al., 2006). Following a prodigious phase of nuclear replication, parasites enter the cytomere stage wherein nuclei distribute peripherally beneath the invaginating inner PPM. Later, the outer PVM disintegrates, releasing merozoites into the host cell cytoplasm. This process *in vitro* leads to cell detachment, followed by the destruction of host cell organelles including the nucleus, and the formation of a host cell membrane-bounded merosome that is able to initiate a blood stage infection (Sturm et al., 2006). Studies with Pb*Δfabl* revealed a striking defect in liver stage maturation. Whereas cell traversal, invasion, and initial development inside a parasitophorous vacuole proceeded normally, late Pb*Δfabl* liver stage parasites displayed a pronounced absence of the MSP1 parasite surface protein in the PPM. Furthermore, these parasites almost completely failed to develop to the cytomere stage, could not normally degrade their PVM, and exhibited an impaired development of merozoites. Pb*Δfabl* parasites also displayed a near total lack of cell detachment and merosome formation (Figure 4; Figure S5). We posit that this developmental arrest explains the attenuated infectivity of Pb*Δfabl* SPZ, as illustrated by their substantially delayed progression to blood stage infection (Table 2). Residual infectivity was nevertheless observed, especially with the higher doses of 10^4 Pb*Δfabl* SPZ that produced blood stage infections in most mice. These “breakthrough” infections were fulminant and lethal, indicating that the few parasites that completed their liver stage development were not attenuated for asexual blood stage growth.

Dr. Stefan Kappe (Seattle Biomedical Research Institute) and colleagues have observed a similar phenotype of late liver stage arrest upon deletion of the FAS-II gene *fabB/F* in *P. yoelii* 17XNL. Their analysis of infected hepatocytes, obtained in BALB/c mice inoculated 44 hr prior with *fabB/F* knockout SPZ, revealed a lack of MSP1 staining and merozoite formation as well as a defect in PVM degradation (based on Hep17 expression), when compared to WT liver stage parasites. In agreement with our observations, no attenuation was evident at other life cycle stages for both *P. yoelii fabB/F* knockout parasites and a further knockout line that carried a deletion of *fabZ*. In contrast to Pb*Δfabl* SPZ, the *P. yoelii fabB/F* knockout line failed to produce breakthrough asexual blood stage infections, even with an inoculum as high as 100,000 salivary gland SPZ (S. Kappe, pers. comm.). This might reflect differences in the virulence of the erythrocytic stages of *P. berghei* ANKA versus *P. yoelii* 17XNL. *P. berghei* ANKA parasites are known to rapidly produce a fulminant, lethal infection starting from low numbers of infected RBC. In contrast, *P. yoelii* 17XNL infections are non-lethal and can be readily resolved by host immune responses. Alternatively, these species might differ in their dependence on FAS-II for successful liver stage development.

Taken together, the FAS-II gene disruption data make a compelling case that *de novo* FA biosynthesis plays a key role in the successful production of the thousands of infectious merozoites produced per infected hepatocyte. While it is possible that FAS-II provides unique (i.e. unsalvageable) FA, the detection of breakthrough infections with Pb*Δfabl* suggests that its role is predominantly to augment levels of salvaged FA to meet metabolic demands. Insights into the potential utilization of FAS-II products are provided by our investigations with

PbΔ*fabI*. These parasites revealed a pronounced deficit in their expression of MSP1, which is anchored to the parasite membrane via GPI moieties. These moieties are enriched in $C_{16:0}$ (palmitic acid), $C_{18:0}$ (stearic acid) and $C_{18:1}$ (oleic acid) (Naik et al., 2000). How could these be produced by the liver stage parasite? Biochemical studies with purified *P. falciparum* FAS-II enzymes provide evidence that this pathway produces predominantly C_{10} to C_{14} FA (Sharma et al., 2007). To modify these species into the saturated and unsaturated FA found in GPI anchors would require the further action of elongases and desaturases (see below), whose activity in liver stage parasites has been detected (Tarun et al., 2008). The inability of PbΔ*fabI* liver stage parasites to form cytomeres and normally degrade their PVM suggests that FAS-II products might also be incorporated into neutral glycerolipids, which have been implicated in intracellular vesicle trafficking, and membrane-resident phospholipids (Palacpac et al., 2004). Likewise, the failure of PbΔ*fabI*-infected hepatocytes to form detached cells suggests that FAS-II products might contribute to parasite manipulation of the phospholipid composition of host cell membranes, a mechanism that appears to subvert immune recognition by liver phagocytes and that correlates with *in vitro* cell detachment (Sturm et al., 2006). This proposed central role of FA in liver stage biology agrees with recent transcriptome data showing that all four *P. yoelii* FAS-II genes are highly expressed in liver stages, as compared to SPZ or asexual blood stages (Tarun et al., 2006). Those studies also revealed upregulation of members of the pyruvate dehydrogenase complex, whose production of acetyl-CoA primes the FAS-II pathway (Mazumdar and Striepen, 2007). These studies evoke the idea of targeting FAS-II enzymes for the development of a novel prophylactic antimalarial drug that clears liver stage infections before they advance to the pathogenic erythrocytic stages.

In contrast to the phenotype of late liver stage arrest observed upon disruption of the FAS-II pathway, other *Plasmodium* gene disruption studies have produced much earlier arrest. Dual disruption of the *P. yoelii* genes *p36* and *p52* (also termed *p36p*), individual knockouts of their orthologs in *P. berghei*, disruption of the *sap1*/*slarp* gene in *P. yoelii* and *P. berghei*, and disruption of the *P. berghei uis4* or *uis3* genes all produced a developmental block within 24–48 hr post invasion ((Aly et al., 2008; Silvie et al., 2008a); and references therein). Of the genetically attenuated SPZ, those that did not cause breakthrough asexual blood stage infections were found to elicit complete protective immunity against challenge with non-attenuated SPZ. We did not perform similar studies because of the finding that PbΔ*fabI* SPZ could produce breakthrough parasitemias. Nevertheless, when compared to the other knockout lines, the delayed demise of PbΔ*fabI* liver stage parasites provides a greater window of antigen presentation, suggesting a potentially enhanced degree of immunogenicity (Jobe et al., 2007). Furthermore, given that the human parasite *P. falciparum* has a prodigious growth phase inside hepatocytes, on the order of 10,000–30,000 merozoites per infected cell as compared to 8,000–10,000 per hepatocyte for *P. berghei* and *P. yoelii* (Verhave and Meis, 1984), one might predict that the inability to produce sufficient levels of FA through *de novo* synthesis could be severely detrimental for *P. falciparum*. Interestingly, the *P. berghei* PVM resident protein UIS3 has been shown to bind L-FABP (liver-fatty acid binding protein), a key mediator of cellular uptake and transport of the FA and lipid species that are abundant in hepatocytes (Furuhashi and Hotamisligil, 2008). This leads us to hypothesize that the disruption of liver stage FA *de novo* synthesis and import might yield potent, genetically attenuated pre-erythrocytic stage vaccines in *Plasmodium* species including *P. falciparum*.

Though the FAS-II pathway appears vitally important to liver stage parasites, the analysis of our PfΔ*fabI* and PbΔ*fabI* lines argues against the earlier hypothesis that this pathway is required for asexual blood stage propagation (Surolia et al., 2004). An alternative explanation of our data would be that another enoyl ACP-reductase might have compensated for the loss of FabI and thereby restore FAS-II functionality to the Δ*fabI* lines during their life cycle. Our bioinformatic search for alternate bacterial enoyl-ACP reductases (FabK, FabL and FabV; (Massengo-Tiasse and Cronan, 2008)) fail to identify any orthologs in *Plasmodium*, although

this does not rule out their potential existence. Nonetheless, the blood and liver stage phenotypes we observe with our Δ*fabI* lines have also been observed by Stefan Kappe and colleagues with transgenic *P. yoelii* parasites that lack *fabB/F* or *fabZ* (pers. comm.). Again, we have not found paralogs of these genes through bioinformatic searches of *Plasmodium* genomes. Our data therefore are consistent with a lack of requirement for the FAS-II pathway in asexual blood stage parasites and support earlier evidence that these stages rely on salvage pathways for the bulk of their FA requirements (Vial and Ancelin, 1992).

In a remarkable body of work, Mi-Ichi *et al.* (Mi-Ichi et al., 2007; Mi-Ichi et al., 2006) found that several combinations including $C_{16:0}/C_{18:0}/C_{18:2,n-6}$ or $C_{16:0}/C_{18:1,n-9}/C_{18:2,n-6}$ were sufficient to replace human serum or Albumax in malaria culture medium and permitted robust parasite growth for over 6 months. These various FA are the predominant species present in human plasma and infected RBC (Mi-Ichi et al., 2006). As per earlier reports (Krishnegowda and Gowda, 2003; Vial and Ancelin, 1992), these authors observed that salvaged FA are predominantly incorporated in an unmodified form into parasite lipids. In addition, they observed FA modification via elongation or desaturation processes. This included the production of $C_{16:0}$ and $C_{18:0}$ from exogenous $[^{14}C]$-$C_{14:0}$ and $[^{14}C]$-$C_{16:0}$ respectively, and desaturation of $C_{18:0}$ to $C_{18:1}$ (Mi-Ichi et al., 2006). In agreement with these findings, we also observed C_{16} and C_{18} FA when incubating *P. falciparum* parasites with $[^{14}C]$-acetate, with no detectable difference between lines harboring or lacking FabI (Figure 3; Figure S2D). We also observed no such incorporation in control uninfected RBC.

P. falciparum asexual blood stage production of radiolabeled C_{16} and C_{18} FA might involve elongases, three of which are encoded by this genome (Lee et al., 2007). The presence of four distinct elongases in the *P. berghei* genome might explain why this species was found to produce C_{12} to C_{24} FA (Figure 3). These ER-resident enzymes are responsible in mammals for producing very long chain FA ($\geq C_{18}$) and in trypanosomes produce C_{10} to C_{18} FA (Jakobsson et al., 2006; Lee et al., 2006). *P. falciparum* asexual blood stages are also capable of modifying FA via desaturation of $C_{16:0}$ and $C_{18:0}$ at the n-9 position, presumably via their Δ–9 desaturase (PFE0555w; (Mi-Ichi et al., 2006)). Another crucial step in the intraerythrocytic modification of imported host FA may involve acyl-CoA synthetase enzymes, which activate acyl chains for entry into FA synthesis, desaturation, and elongation pathways. Members of this gene family are present in 4–12 copies in *Plasmodium* species, and biochemical assays have shown 20–fold higher acyl-CoA synthetase activity in infected versus uninfected RBC (Bethke et al., 2006; Vial and Ancelin, 1992).

FabI has been extensively studied as a candidate drug target for asexual blood stage parasites. Yet our data now argue against the therapeutic potential of this target, and indeed the entire FAS-II pathway, during erythrocytic infection. These data imply that, contrary to earlier suppositions (Ralph et al., 2004; Surolia et al., 2004), asexual blood stage parasites do not require FAS-II activity in the apicoplast. Focusing on FabI, our transgene over-expression and gene disruption studies demonstrate that this is not the target of the antimalarial activity of triclosan (Figure 2 and Figures S1, S2 and S4), despite an earlier report of its inhibition of FA biosynthesis in asexual blood stage parasites and its high affinity for purified enzyme (Perozzo et al., 2002; Surolia and Surolia, 2001). These data agree with studies of *Trypanosoma brucei* parasites that discount FabI as the target of triclosan and have proposed non-specific membrane perturbation as an alternate mode of action (Lee et al., 2007). Our studies nevertheless find that triclosan has activity against *Plasmodium* asexual blood stage parasites, and is efficacious *in vivo* (Figure 1), albeit at concentrations substantially higher than previously reported (Surolia and Surolia, 2001). Further studies are required to elucidate how triclosan acts upon asexual blood stage parasites. In these stages, it is now clear that exogenous FA are essential. We propose that therapeutic strategies to interfere with FA processes in asexual blood stage parasites should focus on import and subsequent modification, presumably

mediated by elongases, the Δ-9 desaturase, and acyl CoA-synthetases. This contrasts with liver stage parasites where interference with FAS-II offers novel perspectives for prophylactic intervention.

EXPERIMENTAL PROCEDURES

Parasite Propagation

P. falciparum lines (Table 1) and *P. berghei* ANKA parasites were propagated as described in the Supplemental Data. All experiments involving rodents were conducted in fully accredited animal facilities and were approved by the Institutional Animal Care and Use Committees of Columbia University, the Albert Einstein College of Medicine, the New York University Medical Center, the University of Miami and the Bernhard Nocht Institute for Tropical Medicine.

Parasite *in vitro* and *in vivo* Drug Susceptibility Assays

The synthesis of triclosan analogs has been previously described ((Freundlich et al., 2007) and references therein). For enzyme inhibition assays, the reaction mixtures contained 50 nM PfFabI, 400 μM NADH and 40 μM NAD^+, and were initiated with 300 μM butyryl-CoA. Inhibition of PfFabI–mediated butyryl-CoA reduction was assessed spectrophotometrically by measuring the oxidation of NADH to NAD^+ at 340 nm (Freundlich et al., 2007). EC_{50} values represent the analog concentration that inhibited maximal PfFabI activity by 50%. Inhibition of *P. falciparum in vitro* or *P. berghei ex vivo* parasite growth was measured using [^{3}H]-hypoxanthine assays, and the IC_{50} values calculated using linear regression (see Supplemental Data). All compounds were tested in duplicate on at least two separate occasions. For *in vivo* efficacy studies, CD-1 mice were infected intraperitoneally on day 0 with 5×10^4 *P. berghei* asexual blood stage parasites. Triclosan (Vita-Pharm, Valhalla, NY) was administered on days 3, 4 and 5 after infection, as two divided doses daily spaced 6 hr apart delivered either PO or SC. Parasitemias were determined from Giemsa-stained smears of tail blood, collected on day 6 and twice a week thereafter until day 31 (see Supplemental Data).

Plasmid Constructs, Parasite Transfections, Nucleic Acid and Protein Analyses, Immunofluorescence Assays, and Structural Elucidation of PbFabI

These are detailed in the Supplemental Data. Primers are listed in Table S2 and transfection plasmids and parasite lines are listed in Table 1.

FA extraction and HPLC analysis

P. falciparum- or *P. berghei*-infected RBC were labeled with [^{14}C]-acetate (10 μCi/ml) for 6 hr or 24 hr respectively at 37°C. Parasite pellets were obtained by saponin lysis, washed twice to remove host cell components, and the FA analyzed by reversed-phase HPLC (see Supplemental Data).

P. berghei Infection of Mosquitoes, Sporozoite Invasion and Cell Traversal Assays, and Analysis of Liver Stage Development

Experimental conditions are detailed in the Supplemental Data.

Determination of *P. berghei* Prepatent Periods in Mice

To determine the *in vivo* infectivity of mutant and control parasite lines, naïve C57BL/6 mice were injected intravenously with 1,000 or 10,000 *P. berghei* salivary gland SPZ, or subjected to the bite of 20 infected mosquitoes that were allowed to probe for 6 min. Asexual blood stage infection was determined by Giemsa-stained blood smears prepared on days 3 through 28 after SPZ inoculation.

Supplementary Material

Refer to Web version on PubMed Central for supplementary material.

Acknowledgements

We thank Drs. Geoff McFadden and Anthony Holder for the *P. falciparum* ACP and *P. yoelii* MSP1 antibodies and the Fidock lab members for helpful discussions. PfERD2 rabbit antiserum (MRA-1) was obtained through the MR4, deposited by John Adams. This work was supported by the National Institutes of Health (P01 AI060342, JCS, DAF, WRJ; and R01 AI056840, PS), the Medicines for Malaria Venture (DAF, JCS, WRJ, DAJ), the Robert A. Welch Foundation (JCS), the Deutsche Forschungsgesellschaft (DFG; 4497/1-2; VH), the Ministère de l'Education Nationale de la Recherche et des Technologies (PG), and the Centre National de la Recherche Scientifique (LK). The authors all declare no conflict of interests.

Glossary

ACP
: acyl carrier protein

CoA
: Coenzyme A

FA
: fatty acids

FAS-II
: type II fatty acid biosynthesis

GPI
: glycosylphosphatidylinositol

HPLC
: High Performance Liquid Chromatography

PO
: per oral

PPM
: parasitophorous plasma membrane

PVM
: parasitophorous vacuole membrane

RBC
: red blood cells

SC
: subcutaneous

SPZ
: sporozoites

WT
: wild type

References

Aly AS, Mikolajczak SA, Rivera HS, Camargo N, Jacobs-Lorena V, Labaied M, Coppens I, Kappe SH. Targeted deletion of SAP1 abolishes the expression of infectivity factors necessary for successful malaria parasite liver infection. Mol Microbiol 2008;69:152–163. [PubMed: 18466298]

Amino R, Giovannini D, Thiberge S, Gueirard P, Boisson B, Dubremetz JF, Prevost MC, Ishino T, Yuda M, Menard R. Host cell traversal is important for progression of the malaria parasite through the dermis to the liver. Cell Host Microbe 2008;3:88–96. [PubMed: 18312843]

Bethke LL, Zilversmit M, Nielsen K, Daily J, Volkman SK, Ndiaye D, Lozovsky ER, Hartl DL, Wirth DF. Duplication, gene conversion, and genetic diversity in the species-specific acyl-CoA synthetase gene family of *Plasmodium falciparum*. Mol Biochem Parasitol 2006;150:10–24. [PubMed: 16860410]

Freundlich JS, Wang F, Tsai HC, Kuo M, Shieh HM, Anderson JW, Nkrumah LJ, Valderramos JC, Yu M, Kumar TR, et al. X-ray structural analysis of *Plasmodium falciparum* enoyl acyl carrier protein reductase as a pathway towards the optimization of triclosan antimalarial efficacy. J Biol Chem 2007;282:25436–25444. [PubMed: 17567585]

Furuhashi M, Hotamisligil GS. Fatty acid-binding proteins: role in metabolic diseases and potential as drug targets. Nat Rev Drug Discov 2008;7:489–503. [PubMed: 18511927]

Gilson PR, Nebl T, Vukcevic D, Moritz RL, Sargeant T, Speed TP, Schofield L, Crabb BS. Identification and stoichiometry of glycosylphosphatidylinositol-anchored membrane proteins of the human malaria parasite *Plasmodium falciparum*. Mol Cell Proteomics 2006;5:1286–1299. [PubMed: 16603573]

Greenwood BM, Fidock DA, Kyle DE, Kappe SH, Alonso PL, Collins FH, Duffy PE. Malaria: progress, perils, and prospects for eradication. J Clin Invest 2008;118:1266–1276. [PubMed: 18382739]

Jakobsson A, Westerberg R, Jacobsson A. Fatty acid elongases in mammals: their regulation and roles in metabolism. Prog Lipid Res 2006;45:237–249. [PubMed: 16564093]

Jobe O, Lumsden J, Mueller AK, Williams J, Silva-Rivera H, Kappe SH, Schwenk RJ, Matuschewski K, Krzych U. Genetically attenuated *Plasmodium berghei* liver stages induce sterile protracted protection that is mediated by major histocompatibility complex Class I-dependent interferon-gamma-producing CD8+ T cells. J Infect Dis 2007;196:599–607. [PubMed: 17624847]

Kapoor M, Gopalakrishnapai J, Surolia N, Surolia A. Mutational analysis of the triclosan-binding region of enoyl-ACP (acyl-carrier protein) reductase from *Plasmodium falciparum*. Biochem J 2004;381:735–741. [PubMed: 15139852]

Krishnegowda G, Gowda DC. Intraerythrocytic *Plasmodium falciparum* incorporates extraneous fatty acids to its lipids without any structural modification. Mol Biochem Parasitol 2003;132:55–58. [PubMed: 14563537]

Lee SH, Stephens JL, Englund PT. A fatty-acid synthesis mechanism specialized for parasitism. Nat Rev Microbiol 2007;5:287–297. [PubMed: 17363967]

Lee SH, Stephens JL, Paul KS, Englund PT. Fatty acid synthesis by elongases in trypanosomes. Cell 2006;126:691–699. [PubMed: 16923389]

Massengo-Tiasse RP, Cronan JE. *Vibrio cholerae* FabV defines a new class of enoyl-acyl carrier protein reductase. J Biol Chem 2008;283:1308–1316. [PubMed: 18032386]

Mazumdar J, Striepen B. Make it or take it: fatty acid metabolism of apicomplexan parasites. Euk Cell 2007;6:1727–1735.

Medica DL, Sinnis P. Quantitative dynamics of *Plasmodium yoelii* sporozoite transmission by infected anopheline mosquitoes. Infect Immun 2005;73:4363–4369. [PubMed: 15972531]

Mi-Ichi F, Kano S, Mitamura T. Oleic acid is indispensable for intraerythrocytic proliferation of *Plasmodium falciparum*. Parasitology 2007;134:1671–1677. [PubMed: 17610764]

Mi-Ichi F, Kita K, Mitamura T. Intraerythrocytic *Plasmodium falciparum* utilize a broad range of serum-derived fatty acids with limited modification for their growth. Parasitology 2006;133:399–410. [PubMed: 16780611]

Mikolajczak SA, Kappe SH. A clash to conquer: the malaria parasite liver infection. Mol Microbiol 2006;62:1499–1506. [PubMed: 17074071]

Muralidharan J, Suguna K, Surolia A, Surolia N. Exploring the interaction energies for the binding of hydroxydiphenyl ethers to enoyl-acyl carrier protein reductases. J Biomol Struct Dyn 2003;20:589–594. [PubMed: 12529157]

Naik RS, Branch OH, Woods AS, Vijaykumar M, Perkins DJ, Nahlen BL, Lal AA, Cotter RJ, Costello CE, Ockenhouse CF, et al. Glycosylphosphatidylinositol anchors of *Plasmodium falciparum*: molecular characterization and naturally elicited antibody response that may provide immunity to malaria pathogenesis. J Exp Med 2000;192:1563–1576. [PubMed: 11104799]

Nkrumah LJ, Muhle RA, Moura PA, Ghosh P, Hatfull GF, Jacobs WR Jr, Fidock DA. Efficient site-specific integration in *Plasmodium falciparum* chromosomes mediated by mycobacteriophage Bxb1 integrase. Nat Methods 2006;3:615–621. [PubMed: 16862136]

Palacpac NM, Hiramine Y, Mi-ichi F, Torii M, Kita K, Hiramatsu R, Horii T, Mitamura T. Developmental-stage-specific triacylglycerol biosynthesis, degradation and trafficking as lipid bodies in *Plasmodium falciparum*-infected erythrocytes. J Cell Sci 2004;117:1469–1480. [PubMed: 15020675]

Perozzo R, Kuo M, bir Singh Sidhu A, Valiyaveettil JT, Bittman R, Jacobs WR Jr, Fidock DA, Sacchettini JC. Structural elucidation of the specificity of the antibacterial agent triclosan for malarial enoyl ACP reductase. J Biol Chem 2002;277:13106–13114. [PubMed: 11792710]

Prudencio M, Rodriguez A, Mota MM. The silent path to thousands of merozoites: the *Plasmodium* liver stage. Nat Rev Microbiol 2006;4:849–856. [PubMed: 17041632]

Ralph SA, van Dooren GG, Waller RF, Crawford MJ, Fraunholz MJ, Foth BJ, Tonkin CJ, Roos DS, McFadden GI. Tropical infectious diseases: metabolic maps and functions of the *Plasmodium falciparum* apicoplast. Nat Rev Microbiol 2004;2:203–216. [PubMed: 15083156]

Scheller LF, Wirtz RA, Azad AF. Susceptibility of different strains of mice to hepatic infection with *Plasmodium berghei*. Infect Immun 1994;62:4844–4847. [PubMed: 7927764]

Sharma S, Sharma SK, Modak R, Karmodiya K, Surolia N, Surolia A. Mass spectrometry-based systems approach for identification of inhibitors of *Plasmodium falciparum* fatty acid synthase. Antimicrob Agents Chemother 2007;51:2552–2558. [PubMed: 17485508]

Silvie O, Goetz K, Matuschewski K. A sporozoite asparagine-rich protein controls initiation of *Plasmodium* liver stage development. PLoS Pathog 2008a;4:e1000086. [PubMed: 18551171]

Silvie O, Mota MM, Matuschewski K, Prudencio M. Interactions of the malaria parasite and its mammalian host. Curr Opin Microbiol 2008b;11:352–359. [PubMed: 18644249]

Sturm A, Amino R, van de Sand C, Regen T, Retzlaff S, Rennenberg A, Krueger A, Pollok JM, Menard R, Heussler VT. Manipulation of host hepatocytes by the malaria parasite for delivery into liver sinusoids. Science 2006;313:1287–1290. [PubMed: 16888102]

Sturm A, Retzlaff S, Franke-Fayard B, Graewe S, Bolte S, Roppenser B, Apfelbacher M, Janse CJ, Heussler VT. Alteration of the parasite membrane and the parasitophorous vacuole membrane during exo-erythrocytic development of malaria parasites. The Protist. 2008in press

Surolia A, Ramya TN, Ramya V, Surolia N. 'FAS't inhibition of malaria. Biochem J 2004;383:401–412. [PubMed: 15315475]

Surolia N, Surolia A. Triclosan offers protection against blood stages of malaria by inhibiting enoyl-ACP reductase of *Plasmodium falciparum*. Nat Med 2001;7:167–173. [PubMed: 11175846]

Tarun AS, Baer K, Dumpit RF, Gray S, Lejarcegui N, Frevert U, Kappe SH. Quantitative isolation and *in vivo* imaging of malaria parasite liver stages. Int J Parasitol 2006;36:1283–1293. [PubMed: 16890231]

Tarun AS, Peng X, Dumpit RF, Ogata Y, Silva-Rivera H, Camargo N, Daly TM, Bergman LW, Kappe SH. A combined transcriptome and proteome survey of malaria parasite liver stages. Proc Natl Acad Sci USA 2008;105:305–310. [PubMed: 18172196]

Verhave JP, Meis JF. The biology of tissue forms and other asexual stages in mammalian plasmodia. Experientia 1984;40:1317–1329. [PubMed: 6391947]

Vial HJ, Ancelin ML. Malarial lipids. An overview Subcell Biochem 1992;18:259–306.

Zhang YM, White SW, Rock CO. Inhibiting bacterial fatty acid synthesis. J Biol Chem 2006;281:17541–17544. [PubMed: 16648134]

A

Activity of triclosan analogs on *Plasmodium falciparum* cultures and purified PfFabI

Series	Number of Compounds	*P. falciparum* 3D7 (μM) Median (min, max)	*P. falciparum* Dd2 (μM) Median (min, max)	Purified PfFabI (nM) Median (min, max)
Triclosan	1	2.8	3.8	73
2'-Position Analogs	15	0.4 (0.1, 14)	0.4 (0.1, 17)	18000 (3300, 35000)
4'-Position Analogs	24	44 (2.1, 120)	49 (3.2, 110)	315 (57, 3000)
4-Position Analogs	4	16 (1.9, 91)	16 (2.6, 54)	3290 (280, 6300)
5-Position Analogs	25	5.6 (1.6, 40)	7.2 (2.5, 45)	290 (38, 33000)
6-Position Analogs	12	2.9 (1.5, 47)	2.4 (1.2, 41)	830 (180, 2900)

Values represent the concentration that produced either 50% inhibition of *P. falciparum* growth (IC_{50}) or purified PfFabI enzymatic activity (EC_{50})
In comparison, chloroquine produced mean IC_{50} values of 30 nM and 280 nM against 3D7 and Dd2 parasites respectively

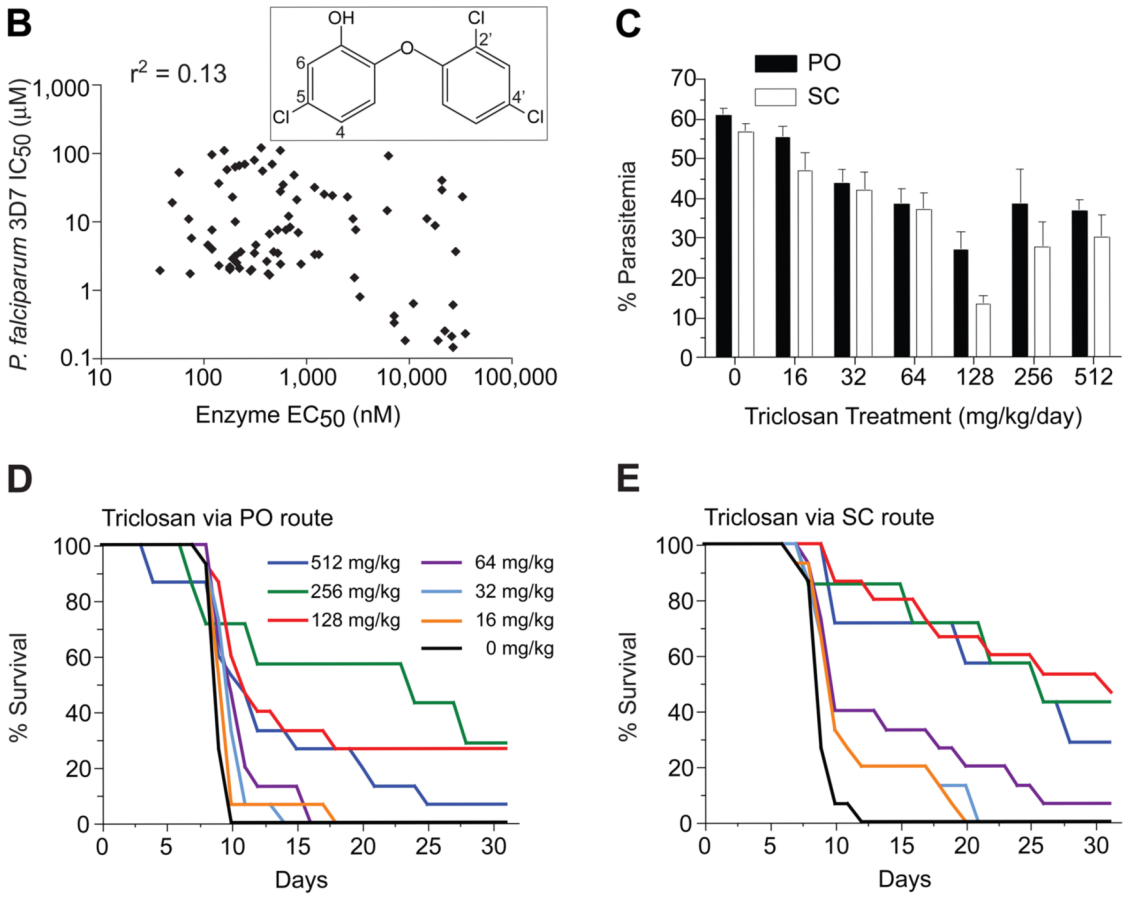

Figure 1. Triclosan Displays *In Vitro* Activity Against *P. falciparum* that Does Not Correlate with Inhibition of FabI and is Less Effective in Curing Rodent Malaria Than Previously Reported

(A) Inhibitory activity of subclasses of triclosan analogs against *P. falciparum* lines and purified PfFabI enzyme. (B) Log scale scatter plot of the activity of triclosan and its analogs against *P. falciparum* 3D7 parasites and purified PfFabI, showing the Pearson r^2 goodness of fit value. The inset shows triclosan (5-chloro-2-(2,4-dichlorophenoxy)phenol) with carbon atoms numbered where substitutions were made. (C) Percent parasitemias plotted for the groups of mice receiving varying doses of triclosan, administered either orally (PO) or subcutaneously (SC) twice daily for three days. Mean values (±SEM) were calculated from

groups of 7–8 mice tested on two separate occasions. (D and E) Kaplan-Meier survival curves for the groups receiving daily triclosan doses as indicated.

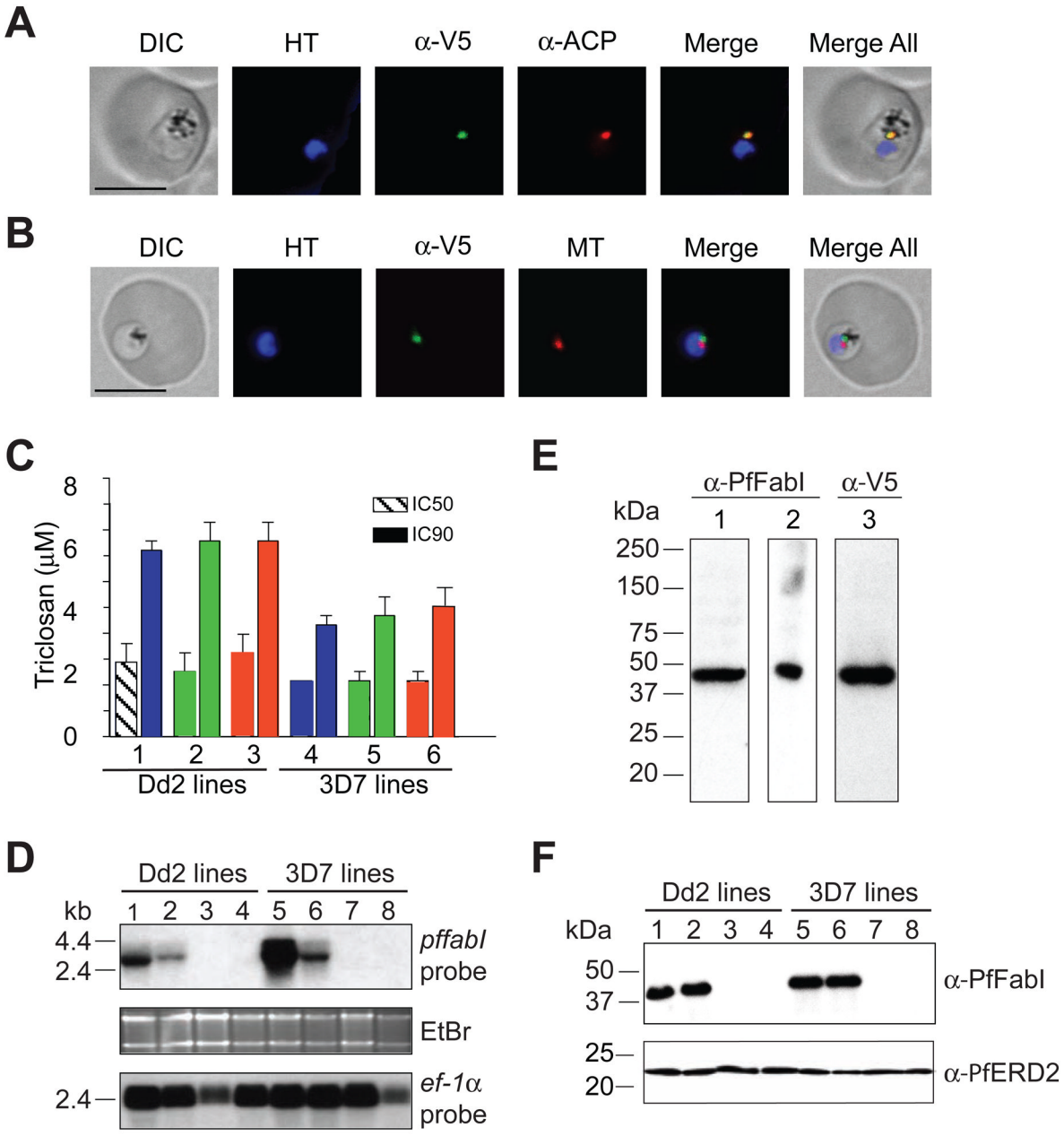

Figure 2. Transgenic Expression of Mutant *pffabI* Does Not Confer Triclosan Resistance *In Vitro*

(A and B) Fluorescence microscopy of Pf*fabI*(A217V)^{Dd2} parasites. Proper targeting of PfFabI-V5 to the apicoplast was illustrated by colocalization of the V5 epitope tag of the mutant protein and acyl carrier protein (ACP). This signal was adjacent to the mitochondrion that was visualized using MitoTracker Red (MT). Scale bar, 5 μm. DIC, Differential Interference Contrast; HT, Hoechst 33342 nuclear dye; α-V5 and α-ACP, antibodies to V5 and ACP. Similar results were obtained with Pf*fabI*(WT)^{Dd2} (data not shown) and with an earlier transgenic Dd2 line that expressed GFP-tagged PfFabI from the same *calmodulin* promoter (Nkrumah et al., 2006). (C) Inhibitory activity of triclosan against *P. falciparum* lines expressing either mutant or WT PfFabI. Data were derived from 3 separate experiments performed in duplicate. Lanes (with mean±SEM IC_{50}, IC_{90} values in μM) 1: Pf*fabI*(A217V)^{Dd2} (2.8±0.7, 6.9±0.4); 2: Pf*fabI*

(WT)^{Dd2} (2.5±0.7; 7.3±0.7); 3: Dd2^{attB} (3.1±0.7, 7.2±0.7); 4: Pf*fabI*(A217V)^{3D7} (2.1±0.4, 4.2 ±0.3); 5: Pf*fabI*(WT)^{3D7} (2.0±0.3, 4.5±0.7); 6: 3D7^{attB} (2.1±0.2, 4.8±0.6). (D) Northern blot analysis showing presence of *pffabI* transcripts only in the lines expressing this transgene from the *calmodulin* promoter. EtBr, ethidium bromide. Lanes 1: Pf*fabI*(A217V)^{Dd2}; 2: Pf*fabI* (WT)^{Dd2}; 3: Dd2^{attB}; 4: Dd2; 5, Pf*fabI*(A217V)^{3D7}; 6, Pf*fabI*(WT)^{3D7}; 7: 3D7^{attB}; 8: 3D7. *ef-1α* was used as a loading control. (E) Evidence that α-PfFabI and α-V5 antibodies recognize the same protein in asexual blood stage parasites expressing *calmodulin* promoter-driven PfFabI. Lanes 1 and 3: Pf*fabI*(A217V)^{Dd2}; 2: Pf*fabI*(WT)^{Dd2} (these lines express PfFabI with a V5 epitope). (F) Western blot analysis showing the detection of PfFabI only in the lines expressing *pffabI* transgenes from the *calmodulin* promoter. α-PfERD2 antibodies were used as a loading control. Lanes 1–8 are the same as in panel D.

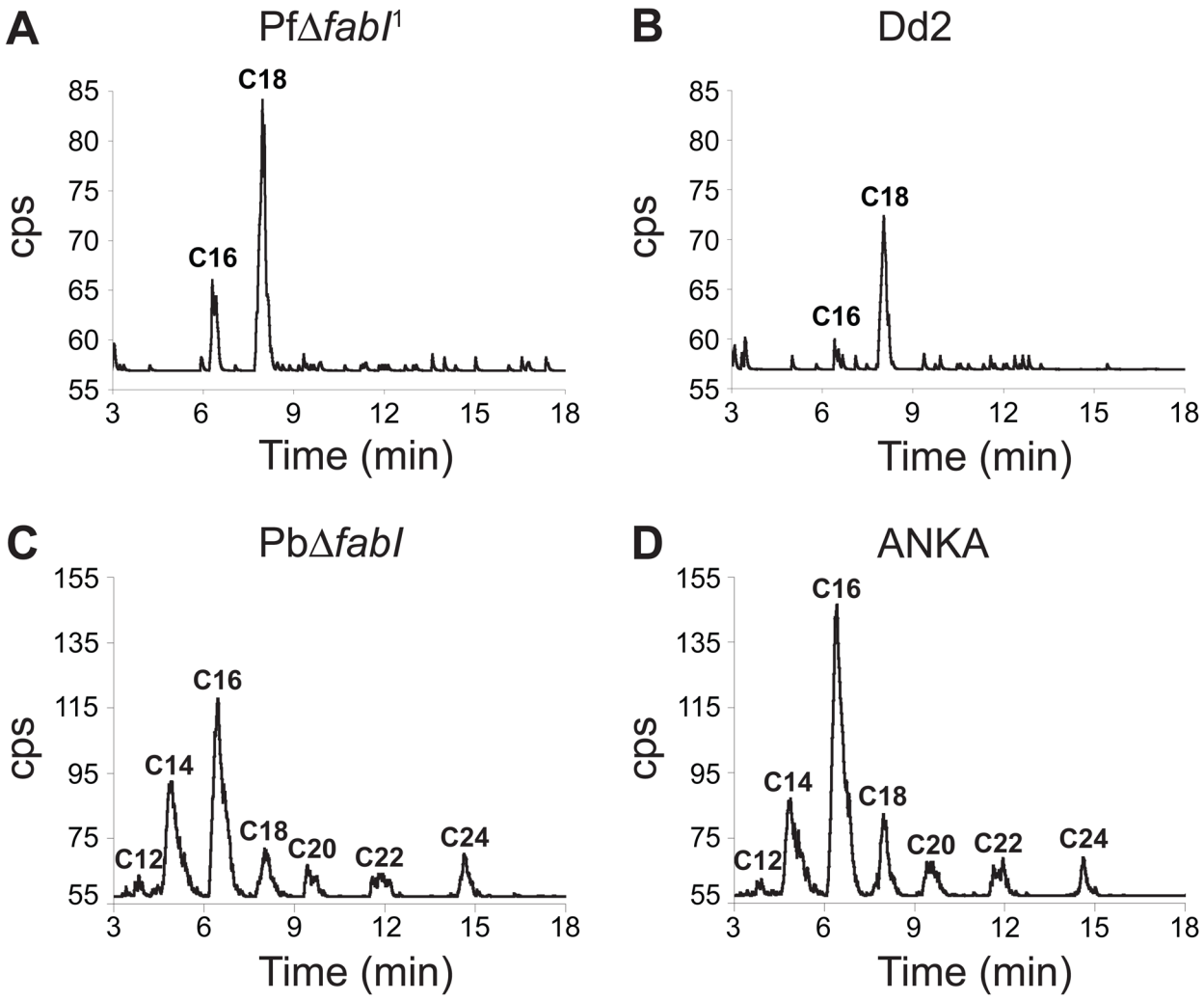

Figure 3. *Plasmodium* Asexual Blood Stage Parasites Modify FA in the Absence of FabI

HPLC analysis of extractable FA *p*-bromophenyacyl esters from *in vitro* cultures of the *P. falciparum* lines (A) PfΔ*fabI*[1] and (B) Dd2, or *ex vivo* cultures of the *P. berghei lines* (C) PbΔ*fabI* and (D) ANKA. Acyl chain lengths are indicated. CPS, counts per second.

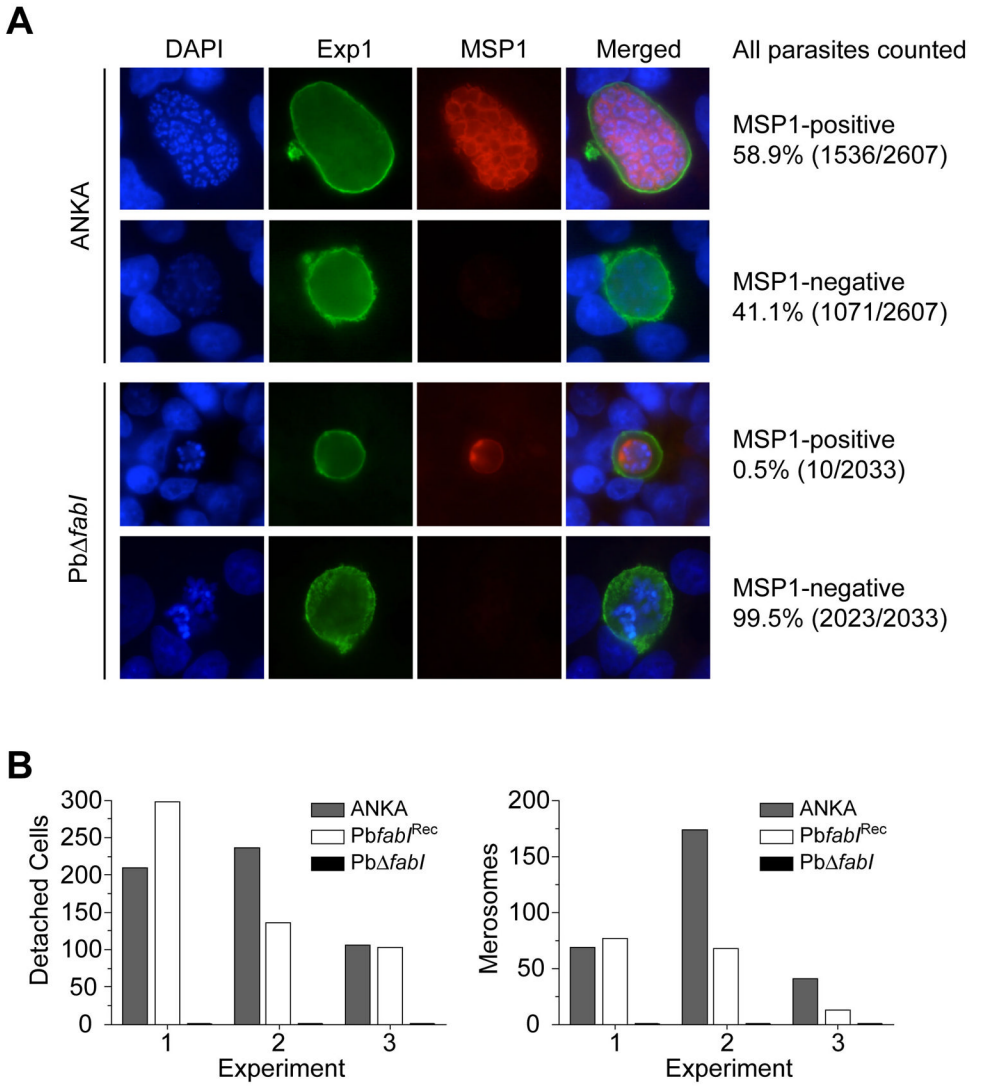

Figure 4. *P. berghei* PbΔ*fabI* Parasites Exhibit a Strongly Impaired Merozoite Development and Fail to Form Detached Cells or Merosomes

(A) IFA results of ANKA and PbΔ*fabI* liver stage parasites grown *in vitro* in HepG2 cells and examined 60 hr post invasion. Parasites were stained with antibodies directed to Exp1 (green) or MSP1 (red), and DAPI (blue) was used to label the parasite and host cell nuclei. (A) Representative images of liver stage parasites developing within an intact PVM, as shown by Exp1 staining as a closed circle around the nuclei. Percentages and numbers of MSP1 positive or negative parasites were collated from three independent experiments. Results show that most ANKA parasites (58.9%) developed normally and produced MSP1-positive merozoites, whereas very few PbΔ*fabI* parasites (0.5%) were MSP1-positive. The upper panel shows a cytomere stage with typical membrane invaginations and arrangements of nuclei close to the PPM. (B) For ANKA, PbΔ*fabI* and Pb*fabI*^{Rec}-infected HepG2 cells, the numbers of detached cells and merosomes were quantified 65 hr post-invasion, in three independent experiments. These revealed a total absence of detached cells and merosomes in PbΔ*fabI* liver stage cultures. Additional representative images are presented in Figure S5.

Table 1

Recombinant and Wild Type Parasite Lines Used in this Study

Parasite line	Species	Recombinant	Transfection plasmid	Endogenous *fabI* gene present	Selectable marker gene[a]	Comment
Pf*fabI*(A217V)^{Dd2}	*P. falciparum*	Yes	*pffabI*(A217V)-V5-attP	Yes	*bsd, hdhfr*	*[1]*
Pf*fabI*(WT)^{Dd2}	*P. falciparum*	Yes	*pffabI*(WT)-V5-attP	Yes	*bsd, hdhfr*	*[2]*
Dd2^{attB}	*P. falciparum*	Yes	None	Yes	*hdhfr*	*[3]*
Dd2	*P. falciparum*	No	None	Yes	None	*[4]*
Pf*fabI*(A217V)^{3D7}	*P. falciparum*	Yes	*pffabI*(A217V)-V5-attP	Yes	*bsd, hdhfr*	*[1]*
Pf*fabI*(WT)^{3D7}	*P. falciparum*	Yes	*pffabI*(WT)-V5-attP	Yes	*bsd, hdhfr*	*[2]*
3D7^{attB}	*P. falciparum*	Yes	None	Yes	*hdhfr*	*[3]*
3D7	*P. falciparum*	No	None	Yes	None	*[4]*
Pf*ΔfabI*^{1}	*P. falciparum*	Yes	pcam-*bsd*-*pffabI*	No	*bsd*	*[5]*
Pf*ΔfabI*^{2}	*P. falciparum*	Yes	pcam-*bsd*-*pffabI*	No	*bsd*	*[5]*
Pb*fabI*	*P. berghei*	Yes	pLitmus28- *pbfabI*	No	*Tgdhfr-ts*	*[6]*
Pb*fabI*^{Rec}	*P. berghei*	Yes	pLitmus28-*pbfabI*^{Rec}	Yes (reinserted)	*Tgdhfr-ts*	*[7]*
ANKA	*P. berghei*	No	None	Yes	None	*[4]*

[a] Selection was performed using blasticidin hydrochloride for *bsd*, WR99210 for *hdhfr*, and pyrimethamine for *Tgdhfr-ts*

1 Expresses mutant *pffabI*(A127V)-V5 transgene from *calmodulin* promoter, integrated into *cg6* attB site

2 Expresses wild type *pffabI*(WT)-V5 transgene from *calmodulin* promoter, integrated into *cg6* attB site

3 Contains attB site integrated into *cg6* locus. Parental line for transfection with attP-containing *pffabI* transgene constructs

4 Wild type non-recombinant line

5 Endogenous *pffabI* locus disrupted by single cross-over homologous recombination, clones 1 and 2

6 Endogenous *pbfabI* locus deleted by double cross-over homologous recombination

7 Endogenous *pbfabI* locus replaced with a wild type copy of *pbfabI* plus the *Tgdhfr-ts* selection cassette

Cell Host Microbe. Author manuscript; available in PMC 2009 December 11.

Table 2

PbΔ*fabI* Sporozoites are Highly Attenuated in their Infectivity for the Host

Experiment	Parasites	Route	Sporozoites	# of infected mice	Prepatent Period (Day)[a]
1	ANKA	Intravenous	1,000	5 of 5	4.8
	Pb*fabI*^{Rec}	Intravenous	1,000	5 of 5	4.6
	PbΔ*fabI*	Intravenous	1,000	2 of 5	8.5
	PbΔ*fabI*	Intravenous	10,000	5 of 5	8.0
2	ANKA	Intravenous	1,000	6 of 6	3.7
	Pb*fabI*^{Rec}	Intravenous	1,000	5 of 5	4.0
	PbΔ*fabI*	Intravenous	1,000	1 of 6	8.0
	PbΔ*fabI*	Intravenous	10,000	5 of 5	7.8
3	ANKA	Intravenous	1,000	5 of 5	3.8
	Pb*fabI*^{Rec}	Intravenous	1,000	5 of 5	4.0
	PbΔ*fabI*	Intravenous	1,000	2 of 5	8.5
	PbΔ*fabI*	Intravenous	10,000	3 of 5	8.3
4	ANKA	mosquito bite	from 20 mosquitoes	5 of 5	4.0
	Pb*fabI*^{Rec}	mosquito bite	from 20 mosquitoes	5 of 5	4.0
	PbΔ*fabI*	mosquito bite	from 20 mosquitoes	4 of 5	9.3

[a] Represents mean number of days after sporozoite inoculation until microscopic detection of blood stage parasites. Mice were examined for blood stage infections daily until day 28. Means were calculated only from the mice that developed a patent infection.